

© IEEE. Personal use of this material is permitted. However, permission to reprint/republish this material for advertising or promotional purposes or for creating new collective works for resale or redistribution to servers or lists, or to reuse any copyrighted component of this work in other works must be obtained from the IEEE.

This material is presented to ensure timely dissemination of scholarly and technical work. Copyright and all rights therein are retained by authors or by other copyright holders. All persons copying this information are expected to adhere to the terms and constraints invoked by each author's copyright. In most cases, these works may not be reposted without the explicit permission of the copyright holder.

Focussing the Beam - A New Laser Illumination Based Data Set Providing Insights to Finger-Vein Recognition

Christof Kauba, Bernhard Prommegger and Andreas Uhl
University of Salzburg
Jakob-Haringer-Str. 2, 5020 Salzburg, AUSTRIA
{ckauba, bprommeg, uhl}@cosy.sbg.ac.at

Abstract

The vascular pattern inside human fingers has become an emerging biometric trait during the last years, commonly denoted as finger vein recognition. However, the number of publicly available data sets is limited. In order to capture a finger vein data set, a suitable scanner device is needed. The design of such a scanner device is crucial if it comes to image quality, robustness against external influences during the capturing process and consequently to a good recognition performance. In this paper we propose two novel, modular designed, multi-purpose finger vein scanners, both able to capture three fingers at once, together with a publicly available finger-vein data set captured with these scanners. One scanner uses common near-infrared LEDs as a light source. The second one is based on a new concept using near-infrared lasers. Near-infrared lasers are not common in finger-vein recognition before despite their advantages especially in touchless operation. Our recognition performance evaluation confirm the good recognition performance that can be achieved using our proposed scanner design and provides some new insights by conducting sex and age-group specific analysis.

1. Introduction

Vascular pattern based recognition (commonly denoted as vein recognition), as a promising new biometric, gains more and more attention and can help to overcome some of the problems existing biometric recognition systems have. Vein based systems rely on the structure of the vascular pattern formed by the blood vessels inside the human body tissue. This pattern only becomes visible in near-infrared (NIR) light. Thus, vein based biometrics provide a good resistance to spoofing and are insensitive to abrasion and skin surface conditions. They achieve good recognition performance while the user convenience is at the same level as for fingerprint systems as long as the scanner is designed in

an open manner. Moreover, a contactless operation is possible and liveness detection can be performed easily [6].

Although, especially hand- and finger-vein based systems are already equipped in commercial products, there is still a lack of comprehensive, public available data sets, which is one of the key factors in order to facilitate research in vascular pattern based biometrics. A major reason for this lack of available data sets is that almost all commercial off-the-shelf finger- and hand-vein scanners do not provide access to the raw vein images they capture. They only output some kind of template in a proprietary format specified by the manufacturer, which is of little use in research. Prior to establishing such a data set, two important things are needed. Most important are the volunteers, who are willing to participate in the data collection, present their fingers to the scanner and donate some of their time while their fingers are scanned. The second most important thing is a scanner device, which provides access to the raw vein images.

A deliberately designed scanner device is crucial for the image quality of the vascular pattern images and consequently, the recognition performance. The first contribution of this paper is our proposed design of two novel multi-purpose finger-vein scanners. Both of our proposed scanners are equipped with transillumination as well as reflected light illumination and are able to capture dorsal and palmar images. They are designed to capture three fingers at a time to speed up the data acquisition process. The scanners differ in the type of their NIR light source: the first one is based on NIR LEDs, while the second one uses NIR lasers. NIR lasers have hardly been used in finger-vein recognition since they were first proposed by Kim et al. [5] in 2009. The main advantage of lasers over LEDs is an increased range of possible vertical finger movement without impacting the image quality. This becomes important as soon as the finger is desired not to touch the sensor's surface and thus especially if it comes to touchless operation. This paper covers the main aspects of our scanner design. The details of the scanner design, including all construction plans, schematics, parts lists and the software will be

made publicly available as an open-hardware project. Other researchers interested in finger-vein biometrics can benefit from our open-source scanner design, build a scanner on their own and capture finger-vein images. By providing their captured data, they can help in establishing an extensive, publicly available finger-vein data set and thus help in stimulating research on vascular biometrics. Such an extensive data set is especially vital in order to develop efficient (in terms of runtime) finger-vein identification and finger-vein indexing schemes.

The main contribution of this paper is the data set itself, which was captured utilising our two finger-vein scanners. This new, publicly available, dorsal finger-vein data set consists of two sub sets: one for each of our proposed two scanners. To the best of our knowledge there is neither a finger-vein data set which was acquired using NIR laser illumination nor an extensive, publicly available, data set containing dorsal images. Our data set provides high resolution dorsal finger-vein images of 360 individual fingers together with additional information about the 60 subjects. It is currently being extended by capturing additional subjects and is expected to grow further due to our plans to make the scanner hardware an open-source project.

The performance evaluation based on some well-established finger-vein recognition algorithms confirms the good recognition performance that can be achieved using our data set, both the LED and the laser scanner one. Beyond the baseline performance results, a subgroup specific analysis of the recognition performance is carried out. The whole data set is divided into 2 sex specific subgroups as well as 3 age specific ones. We did not come across any other finger-vein recognition paper that covers such a subgroup specific performance evaluation so far. The subgroup specific results indicate that there is no significant difference in the recognition performance for male and female subjects as well as among the different age groups. Finally, the cross-sensor (LED vs. laser) recognition performance is evaluated and an image quality analysis using several no reference image quality metrics is performed.

The rest of this paper is organised as follows: Section 2 explains the principle of a finger-vein scanner in general, followed by the details about the two proposed finger-vein scanning devices. In Section 3 at first an overview of available finger-vein data sets, including all important details, is given. This is followed by a detailed description of our new finger-vein data set. Section 4 outlines the experimental setup, including the recognition tool-chain as well as the evaluation protocol and gives the performance evaluation results together with a results discussion. Section 5 concludes this paper along with an outlook on future work.

2. Finger-Vein Scanners

Finger-vein biometrics rely on the structure of the vascular pattern inside the fingers of a human. To be able to extract meaningful features of this vascular structure at first the blood vessels inside the human body tissue have to be made visible. The blood vessels can be rendered visible (as dark lines in the images) due to the fact that the haemoglobin contained in the blood flowing through the vessels absorbs NIR light while the surrounding tissue is semi-permeable. Hence, the crucial components of a finger-vein scanner are an NIR sensitive camera and some kind of NIR light source, the latter typically consists of NIR LEDs with wavelengths between 750 nm and 950 nm. Usually either an NIR pass-through filter is added to the camera or the scanner is enclosed in an optically opaque box in order to reduce the influence of ambient light.

Based on the positioning of the illuminator relative to the camera and the finger, there are two types of illumination:

1. Transillumination, where the camera and the illuminator are positioned on opposite sides of the finger. The light penetrates the skin and tissue of the finger and gets captured by the camera as it emerges.
2. Reflected light, where the camera and the illuminator are positioned on the same side of the finger. The light originates from the light source, gets reflected at the finger's surface and tissue and is captured by the camera.

A further distinction can be made based on the side of the finger where the camera is positioned or the images is taken from, respectively: palmar (also called ventral), where the images are taken from the palm side of the hand and dorsal, where the images are taken from the back side of the hand.

In finger-vein recognition usually palmar images are captured using transillumination. Our proposed scanners are multi-purpose finger-vein scanners, i.e. they are able to capture dorsal as well as palmar images and apply transillumination as well as reflected light illumination. Thanks to its modular design it is easy to change, replace, modify or improve individual parts of the scanner while keeping its basic structure.

2.1. PLUS OpenVein LED Based Scanner

The LED based version of the PLUS OpenVein finger-vein scanner can be seen in Figure 1. The image sensor is an NIR enhanced industrial camera (IDS Imaging UI-ML1240-NIR) equipped with a Fujifilm HF9HA-1B 9 mm lens in combination with a MIDOPT FIL LP830/27 NIR pass-through filter. The transillumination light source consists of 3 stripes (one underneath each finger) of 8 Osram SFH-4253-Z LEDs each. An LED ring consisting of 8 850

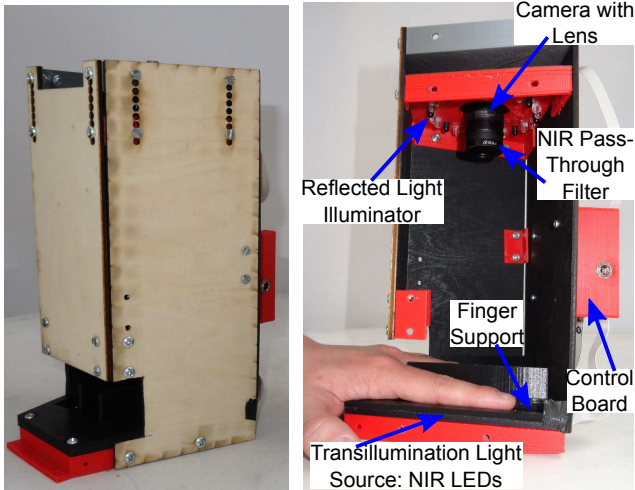


Figure 1. PLUS OpenVein three-finger vein scanner LED version

nm LEDs, 8 950 nm LEDs and 8 daylight LEDs for capturing reflected light images is situated on top of the device. To assist in positioning of the finger, the lower part contains a custom 3D printed finger support which serves as a bracket for the 3 LED stripes too. The control board is located on the back plate of the scanner. This scanner is designed to capture 3 fingers (index, middle and ring finger) at once. It is able to capture both palmar and dorsal (by rotating the hand) as well as transillumination and reflected light finger vein images. The whole scanner is built into a wooden housing to improve stability. The outside dimensions of the scanner are $146 \times 175 \times 258 \text{ mm}$. All the housing parts, the 3D printed parts and the control boards were designed by ourselves. The acquisition time for one image is about 3 s (containing three fingers). Figure 6 bottom shows some example images captured with this scanner.

The scanner has an integrated control board which enables the individual brightness control of each of the transillumination LEDs. The capturing software uses an automatic brightness control algorithm to achieve an optimal image contrast and quality. This is done iteratively by comparing the average grey level of the image area around each LED centre ($GL_{current}$) with a pre-configured target value (GL_{target}). Initially all LEDs are set to half of the maximum intensity (I_{max}). The intensity correction is then done according to: $corr = \frac{GL_{target} - GL_{current}}{GL_{max}} \cdot \frac{I_{max}}{2 \cdot n}$, where GL_{max} is the maximum grey value and n is the current iteration. The LED centre positions are pre-configured too. Each of the 3 reflected light illuminators can be brightness controlled as a whole as well (not the individual LEDs).

2.2. PLUS OpenVein Laser Based Scanner

This scanner is the first finger-vein scanner that uses NIR laser diodes instead of NIR LEDs for transillumination. The

main parts (camera, reflected light source, finger support and housing) of the laser based scanner are the same as for the LED version except the illuminator and the control board. The transillumination light source consists of 3x 5 DLC-180-500-9T5 808 nm 300 mW laser diodes including a control PCB and a housing with an adjustable lens to focus the laser beam (subsequently called laser module). An image of the scanner can be seen in Figure 1. The height of laser based scanner is larger than the LED version (outside dimension are: $146 \times 175 \times 306 \text{ mm}$) because the laser modules are bigger than the LEDs.

An NIR illuminator based on laser modules instead of LEDs exhibits several advantages in the transillumination setting. First of all the laser modules have a very narrow radiation angle. If LEDs are used, the finger has to be placed close to the light source. As soon as the finger does not directly touch the sensor surface most of the light emission passes alongside and outside the finger, not through the finger. Thus, the finger boundaries appear too bright while the interesting regions of the finger containing the blood vessels exhibit little contrast leading to a lower vein image quality in general, which can be seen in the bottom row of Figure 6 and in detail in Figure 3. Depending on the radiation angle of the LED this gets worse the farther away the finger is from the illuminator, implying problems especially if the distance between illuminator and finger cannot be easily controlled. Figure 5 shows some example images captured with our scanners. The distance between the finger and the scanner surface varies from 0mm (directly on the scanner surface), 20 mm and 40 mm. The images captured with the LED based scanner (left part of the figure) clearly show more bright areas around the finger boundaries and less image contrast of the vein region the further away the finger is from the scanner surface, while the laser based scanner (images in right part of the figure) is still able to maintain a good image contrast in the vein region. This is one of the main problems if it comes to touchless finger-vein scanners. The narrow radiation angle of the laser modules enables an increased range of vertical finger movement (see Figure 4 for an illustration) without lowering the overall vein image contrast and quality. This is a key requirement for real touchless operation of a finger-vein scanner. Thus, the design of a touchless finger-vein scanner becomes feasible or at least less complex by utilising laser modules. Kim et al. [5] were the first to propose the use of NIR lasers instead of NIR LEDs in 2009. They exploited the increased range of vertical finger movement and higher illuminous flux compared to LEDs in their touchless finger-vein scanner. In contrast to our design they used only one NIR laser in combination with a laser line generator lens. They made a real-time camera control software to achieve an optimal image contrast instead of controlling the laser's illumination intensity. Their acquired data set consisting of 200 images

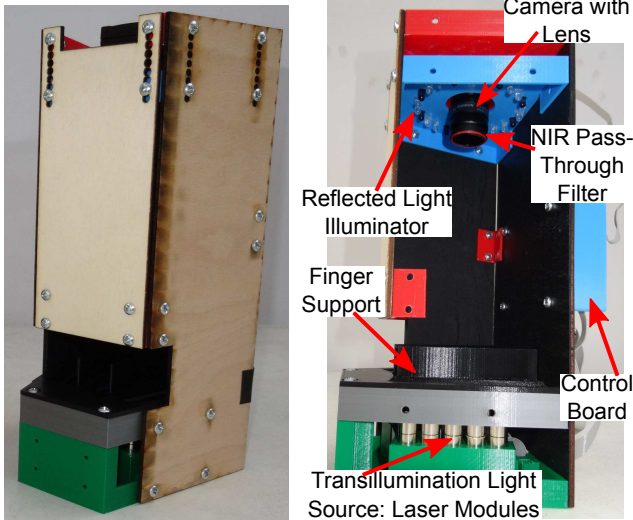


Figure 2. PLUS OpenVein three-finger vein scanner laser version

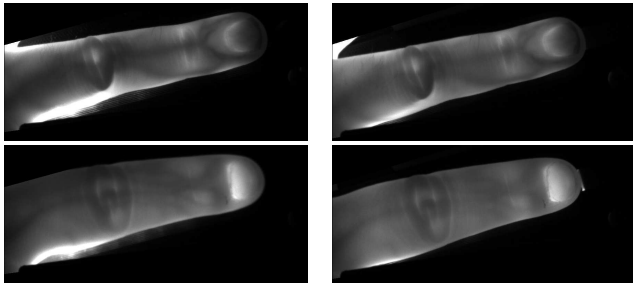


Figure 3. Comparison of LED (left) and laser (right) illumination. Note the bright spots along the left bottom part of the finger for the LED scanner images which are reduced using the laser illumination.

captured from 10 different subjects has not been published. Another advantage of NIR laser modules is that the emission spectrum of the laser modules is narrower compared to LEDs. This enables the use of narrow band-pass filters instead of NIR long-pass filters (filters all wavelengths below the cut-off frequency but all frequencies above it will pass unaffected) to further reduce the influence of ambient illumination. The disadvantages of laser modules include the higher current consumption (400 mA compared to 70 mA for an LED), bigger size and the higher costs compared to LEDs.

3. PLUSVein-FV3 Dorsal Finger-Vein Data Set

Table 1 lists some details of the the 8 publicly available finger vein data sets we found so far, including the number of subjects (subjs), the number of fingers per subject that were captured (fings), the total number of images (imgs) as well as if the images are captured from the palmar or dorsal side (dors/palm). Furthermore, the number of ses-

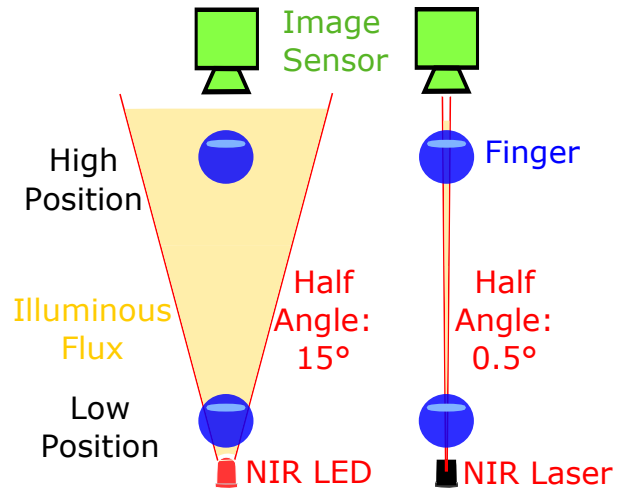


Figure 4. Illumination issues due to vertical finger movement: for usual LEDs (depicted here is an LED with a radiation half angle of 15°) the further away the finger is from the illuminator, the higher the amount of illuminous flux that is outside the finger. The more illuminous flux outside the finger, the less image contrast and vein visibility. Laser modules have a narrow radiation angle, thus the illuminous flux outside the finger remains 0 if the finger is moved in y-direction.

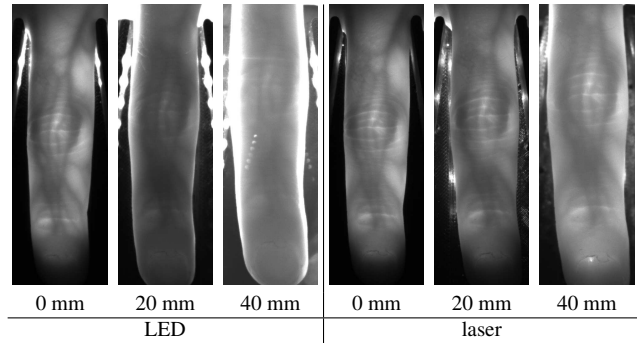


Figure 5. Finger-vein images captured with our scanners showing illumination issues due to vertical finger movement: note the bright areas along the finger boundaries and the reduced contrast of the vein region the further away the finger gets from the scanner surface for the LED scanner images (left) compared to the laser scanners ones (right) which still exhibit enough image contrast.

sions (sess), the image resolution and more important the effective resolution of the visible finger area inside the images (finger w*h) as well as the type of camera and the illumination type is given if this information was available. The last row lists our new finger-vein data set.

This table clearly shows that all of these data sets except the PROTECT Multimodal Database [16] are palmar finger-vein data sets. Raghavendra and Busch [13] did some experiments on dorsal finger veins but their data set has never been published. Moreover, for all of these data sets, NIR

name	subs	fings	imgs	dors/palm	sess	resolution	finger w*h	camera	illumination
UTFVP [15]	60	6	1440	palmar	2	672 × 380	672 × 240	C-Cam BCi5	850 nm LEDs
SDUMLA-HMT [19]	106	6	3816	palmar	1	320 × 240	320 × 130	NIR CCD 900nm	890 nm LEDs
FV-USM [1]	123	4	5940	palmar	2	640 × 480	170 × 450	Sony PSEye cam	850 nm LEDs
VERA FingerVein [14]	110	2	440	palmar	2	665 × 250	650 × 240	C-Cam BCi5	850 nm LEDs
MMCBNU_6000 [9]	100	6	6000	palmar	1	640 × 480	640 × 240	-	850 nm LEDs
THU-FVFDI [18]	610	2	6540	palmar	2	720 × 576	200 × 500	camera + NIR filter	890 nm LEDs
HKPU-FID [6]	156	2	3132	palmar	2	512 × 256	512 × 190	NIR camera	850 nm LEDs
PMMDB-FV [16]	20	4	240	dorsal	1	1280 × 440	1120 × 400	UI-ML1240-NIR	850 nm LEDs
PLUSVein-FV3	60	6	3600	dorsal	1	1280 × 1024	200 × 750	UI-ML1240-NIR	LEDs/laser

Table 1. Available finger-vein data sets

LEDs were used as light source. The main contributions of our data set are:

1. A comprehensive dorsal finger-vein data set. We aimed at optimising the acquisition set-up to achieve a high and consistent image quality in order to obtain a good recognition performance.
2. Images captured using two scanners: one with NIR LED based illumination and one with NIR laser module based illumination.
3. Subjects' metadata enabling sub-group specific analysis (e.g. sex and age group as we performed in this paper).

3.1. Data Set Description

The PLUSVein-FV3 finger-vein data set consists of 2 subsets: one dorsal finger-vein subset captured with the LED based scanner and one dorsal finger-vein subset captured with the laser module based scanner. There are the same 60 subjects in each of the 2 subsets. 6 fingers (left and right index, middle and ring finger) and 5 images per finger in 1 session were captured. So each subset consists of 360 individual fingers. Each scanner captures 3 fingers at a time. Thus, each subset contains 600 raw finger-vein images. Some of these example images can be seen in Figure 6. The images are then separated into 3 parts, corresponding to index, middle and ring finger, respectively. Hence, there are effectively 1800 images in each subset and 3600 images in the data set in total. 25 of the subjects are female, 35 are male. The youngest subject was 18, the oldest one 79. The subjects are from 11 different countries.

The raw images have a resolution of 1280×1024 pixels and are stored in 8 bit greyscale png format. The separated images have a resolution of 420×1024 pixels and the visible area of the finger inside the images is about 200×750 pixels per finger. The data set is publicly available for research purposes and can be downloaded at: <http://www.wavelab.at/sources/PLUSVein-FV3>. It is still being extended and is expected to contain more than 100 subjects until the end of 2018.

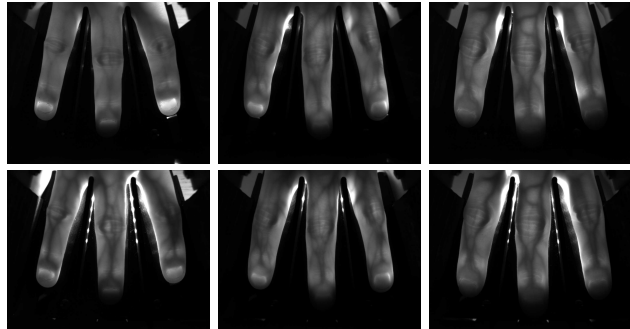


Figure 6. Scanner example images, laser (top) and LED (bottom)

4. Performance Evaluation

In the following the finger-vein processing tool-chain and the evaluation protocol are described. Then the experimental results are given and discussed.

4.1. Processing Tool-Chain

The finger-vein processing tool-chain consists of ROI (region of interest) extraction, preprocessing, feature extraction and comparison. We opted for simple binarisation type feature extraction methods as well as one key-point based method (SIFT based) to have a complimentary feature type too. If these simple recognition schemes perform well on our data set, more recent and more sophisticated recognition schemes will certainly perform even better. Implementations of all of the methods we used are publicly available.

ROI Extraction At first the input image is split into 3 parts, corresponding to index, middle and ring finger, respectively. This can be done using fixed boundary lines. Afterwards each image is processed individually. Prior to the extraction of the ROI, the finger outline is detected by the help of edge detection algorithms. Then a straight centre line is fitted into the finger. Based on this centre line, the finger is aligned (rotated and shifted) such that it is in upright position in the middle of the image. Then the area outside the finger is masked out (pixels set to black). Then a rectangular ROI is fit inside the finger area. The ROI images

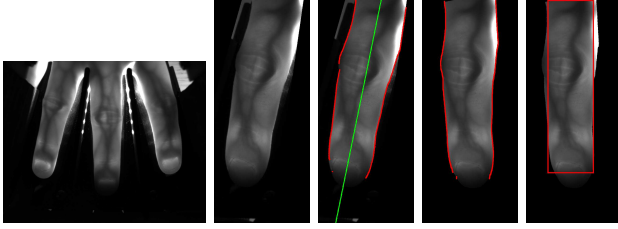


Figure 7. ROI extraction process, from left to right: input image, left finger separated, finger outline and centre line detection, finger aligned and masked, ROI boundary

have a size of 192×736 pixels. The single steps of the ROI extraction are depicted in Figure 7.

Preprocessing To improve the image contrast and the visibility of the vein pattern **CLAHE** [22], which is the most prevalent and simple technique, in combination with **High Frequency Emphasis Filtering (HFE)** [21] and filtering with a **Circular Gabor Filter (CGF)** as proposed by Zhang and Yang [20] are applied. Furthermore, the images are resized to half of its original size, which not only speeds up the comparison process but further improves the results due to intrinsic denoising. For more details on the preprocessing methods the interested reader is referred to the authors’ original publications..

Feature Extraction and Comparison The first three of the following techniques aim to extract the vein pattern from the background resulting in a binary template image followed by a comparison of these binary templates using a correlation measure.

Maximum Curvature (MC) [12] aims to emphasise only the centre lines of the veins, making it insensitive to varying vein widths. The first step is the extraction of the centre positions of the veins. Afterwards a score according to the width and curvature of the vein region is assigned to each centre position and recorded in a matrix called locus space. Due to noise or other distortions some pixels may not have been classified correctly at the first step, thus the centre positions of the veins are connected using a filtering operation. Finally binarisation is done by thresholding using the median of the locus space.

Principal Curvature (PC) [2]): At first the gradient field of the image is calculated. Hard thresholding is done to filter out small noise components and then the gradient at each pixel is normalised to 1 to get a normalised gradient field. This is smoothed by applying a Gaussian filter. The next step is the actual principal curvature calculation, obtained from the Eigenvalues of the Hessian matrix at each pixel. Only the bigger Eigenvalue, corresponding to the maximum curvature, is used. The last step is a binarisation of the prin-

cipal curvature values to get the binary vein output image.

Gabor Filter (GF) [6]: The image is filtered using a filter bank consisting of several 2D even symmetric Gabor filters with different orientations, resulting in several feature images. The final vein feature image is obtained by fusing all these single images, which is then post-processed using morphological operations to remove noise.

For comparing the binary feature images we adopted the approach of Miura et al. [12]. As the input images are neither registered to each other nor aligned vertically, the correlation between the input image and x- and y-direction shifted versions of the reference image is calculated. The maximum of these correlation values is normalised and then used as final comparison score.

In addition to the techniques described above, the fourth technique is a key-point based one. Key-point based techniques try to use information from the most discriminative points as well as considering the neighbourhood and context information of these points by extracting key-points and assigning a descriptor to each key-point. We used a **SIFT** [8] based technique with additional key-point filtering along the finger boundaries as proposed by Kauba et al. [4].

4.2. Evaluation Protocol

To quantify the performance, the EER as well as the FMR1000 (the lowest $FNMR$ for $FMR \leq 0.1\%$) and the ZeroFMR (the lowest $FNMR$ for $FMR = 0\%$) are used. We followed the test protocol of the FVC2004 [10]. For calculating the genuine scores, all possible genuine comparisons are performed, which are $62 \cdot 6 \cdot \frac{5-4}{2} = 3600$ comparisons. For calculating the impostor scores, only the first image of a finger is compared against the first image of all other fingers, resulting in $6 \cdot \frac{60-59}{2} = 10620$ comparisons, so 14220 comparisons in total. All result values are given in percentage terms, e.g. 1.43 means 1.43%. A public implementation of the complete processing tool-chain as well as the score and detailed results are available at: <http://www.wavelab.at/sources/Kauba18c>.

4.3. Baseline Performance Results

Table 2 shows the baseline recognition performance results for all 4 tested finger-vein recognition schemes and both scanner types, laser and LED. All of the 4 quite simple finger-vein recognition schemes achieve a competitive recognition performance in terms of EER, FMR1000 as well as ZeroFMR on both, the laser and the LED scanner data set. The DET plots for the laser and the LED scanner can be found in Figure 8 left and right, respectively. Regarding the laser scanner data set, MC performs best achieving an EER of 0.028%, followed by SIFT and PC while GF performs worst. On the LED scanner data set, PC performs slightly better than MC (in terms of ZeroFMR), both having an EER of 0.028%. SIFT is ranked third while GF again performs

		MC	PC	SIFT	GF
laser	EER	0.028	0.331	0.111	0.523
	FMR1000	0.028	0.444	0.111	0.694
	ZeroFMR	0.028	0.694	0.361	1.306
LED	EER	0.028	0.028	0.117	0.336
	FMR1000	0.028	0.028	0.139	0.444
	ZeroFMR	0.083	0.056	0.361	0.917

Table 2. Baseline performance results (the best results per illumination type are highlighted **bold**)

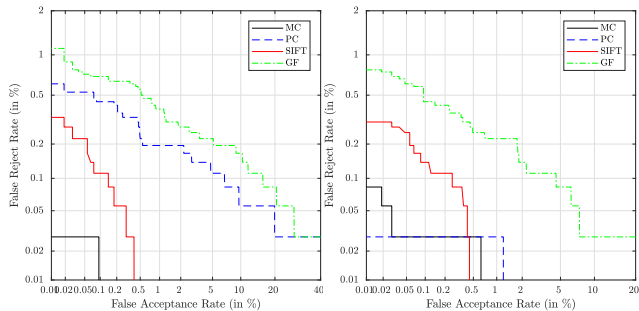


Figure 8. DET plot for laser scanner (left) and LED (right)

worst. Note that due to the limited number of comparison scores (14220) the resolution of the DET curve is limited. Thus, the DET curve of MC and the one of PC for the LED scanner shows a straight line between 0.01% and 0.1% (0.6% for MC on the LED scanner and 1.2% for PC on the LED scanner, respectively). Consequently, the EER could be any value in between 0.028% and 0.1%/0.6%/1.2%, respectively. We decided to report the lowest possible FRR as EER in those cases. In our scanner set-up, where the fingers are placed directly above the illumination source, the tested recognition schemes perform slightly better on the LED scanner data set than on the laser one, especially PC and GF. However, the laser based scanner has its main advantage in terms of recognition performance if the finger is not placed directly on the scanner surface but located a few centimetres away from it (touchless operation).

4.4. Cross-Sensor Comparison Performance

The cross-sensor recognition performance results are given in Tab. 3. MC performs best if it comes to cross-sensor comparison achieving a competitive EER of 0.288%. This time GF performs second best, followed by PC while SIFT performs worst. In terms of relative performance degradation ($\frac{EER_{i,cross} - EER_{i,single}}{EER_{i,single}} \cdot 100\%$, where $EER_{i,cross}$ is the cross-sensor comparison EER for the i -th recognition scheme and $EER_{i,single}$ is the lower of the two single sensor performances for the corresponding recognition scheme), MC's performance dropped by about 930%. PC's performance dropped by 740%, the one of SIFT by 2340% and the one of GF only by 160% in terms of relative EER increase. According to these relative per-

	MC	PC	SIFT	GF
EER	0.288	2.775	2.86	1.353
FMR1000	0.478	5.078	5.622	3.522
ZeroFMR	1.267	6.522	7.689	8.144

Table 3. Cross-sensor (LED vs. laser) comparison performance results

		male		female	
		MC	SIFT	MC	SIFT
nr. of subjects		35		25	
laser	EER	0.0	0.038	0.061	0.122
	FMR1000	0.0	0.286	0.067	0.2
	ZeroFMR	0.0	0.429	0.067	0.4
LED	EER	0.089	0.052	0.0	0.211
	FMR1000	0.048	0.048	0.0	0.267
	ZeroFMR	0.95	0.048	0.0	0.533

Table 4. Sex subgroup specific results

formance drops GF can handle the cross-sensor comparison best. However, MC still performs best in terms of absolute performance values in the cross-sensor comparison. Summing up, the cross-sensor comparison lowers the recognition performance but is still usable in practical deployments of finger-vein scanners, especially if it comes to MC.

4.5. Sex and Age Group Specific Analysis

In addition to the baseline performance evaluation we also conducted a subset specific analysis. Therefore, we divided the total data set into 2 sex (male/female) and 3 age group (< 30 / $\geq 30 < 40$ / ≥ 40) specific subsets. To keep the tables and plots clear, only the results of MC and SIFT are depicted. PC and GF follow the same trend. The sex subgroup specific results are given in table 4. While the general performance (including male and female subjects) in terms of EER for MC using the LED scanner data is 0.028%, for the male subset it is 0.089%, whereas for the female one it is 0%. For SIFT the situation is completely opposite: the baseline EER for the LED scanner data is 0.117%, for the male subset it is 0.052% and for the female one it is 0.211%. Regarding the laser scanner, male subjects achieve a slightly better recognition performance than female ones for both, MC and SIFT. Overall, there is no substantial difference between male and female subjects regarding the recognition performance using our finger-vein recognition system including the scanner hardware and the recognition tool-chain.

The age-group specific results are listed in table 5. It can be seen that for the LED scanner the EER as well as the FMR1000 and the ZeroFMR are all 0%, i.e. the best recognition performance that can be achieved. Consequently, there is no difference between the three age subgroups, i.e. the finger-vein recognition system's performance is inde-

		< 30		$\geq 30 < 40$		≥ 40	
		MC	SIFT	MC	SIFT	MC	SIFT
nr. of subjects		19		21		20	
laser	EER	0.0	0.0	0.0	0.0	0.0	0.0
	FMR1000	0.0	0.0	0.0	0.0	0.0	0.0
	ZeroFMR	0.0	0.0	0.0	0.0	0.0	0.0
LED	EER	0.0	0.0	0.0	0.0	0.0	0.0
	FMR1000	0.0	0.0	0.0	0.0	0.0	0.0
	ZeroFMR	0.0	0.0	0.0	0.0	0.0	0.0

Table 5. Age subgroup specific results

metric	BIQAA	SSEQ	GCF	Wang17
laser	0.00461	28.5888	1.289	0.32679
LED	0.00423	36.4295	1.419	0.30035

Table 6. Image quality evaluation results, BIQAA values are in the range of [0, 1], SSEQ in [0, 100], GCF in [0, 8] and Wang17 in [0, 1]. Higher values correspond to higher image quality, except for SSEQ where 0 is the best quality.

pendent of the subject’s age. The results for the laser scanner are in line with the LED ones. Note that this is only a first indicator as the number of subjects/fingers in each of the subgroups is low. In order to arrive at a more profound statement, a larger data set is needed.

4.6. Image Quality Assessment

The finger-vein images were analysed using 2 general image quality metrics (BIQAA [3] and SSEQ [7]). BIQAA and SSEQ were selected as they have been proved to be well suited for natural scene images. As they are based on image entropies they should perform well using arbitrary, not necessarily natural scene images, too. Moreover, GCF [11] was selected as it is a general image contrast metric and thus independent of the image content. With the help of GCF the image contrast can be quantified exclusively disregarding the actual image content. As we aim to quantify the image quality of finger-vein images, of course a vein specific NIR image quality metric, Wang17 [17] was included as well. The image quality assessment results, listed in Tab. 6 are diverse. The recognition performance of the LED scanner is superior compared to the laser one. However, only GCF indicated that the LED images exhibit a higher image quality while BIQAA, SSEQ and Wang17 indicate the contrary. Hence, a reliable prediction of the recognition performance based on the assessed image quality is not possible.

5. Conclusion and Future Work

Two new, modular designed, multi-purpose finger-vein scanners have been proposed. The first one is based on widely used NIR LED illumination while the second one uses NIR lasers. NIR lasers have hardly been used in finger-vein recognition despite their advantages over LEDs, espe-

cially if it comes to touchless operation. Due to the narrow radiation angle of the lasers they enable an increased range of vertical finger movement without lowering the image contrast and overall image quality. A new dorsal finger-vein data set captured by utilising our two proposed scanners has been established. This data set contains 360 individual fingers (60 subjects and 6 fingers each), is publicly available for research purposes and can be downloaded at: <http://www.wavelab.at/sources/PLUSVein-FV3>.

The performance evaluation on our new data set confirms the decent recognition performance that can be achieved using our proposed scanner design, both the LED and the laser version and in the cross-sensor comparison scenario as well. Even the selected simple but well-established finger-vein recognition schemes arrived at quite a remarkable performance. In our set-up, where the finger is placed directly on top of the illumination source, the LED based scanner is able to compete and even slightly outperform the laser based version. However, this situation changes if the finger is placed a few centimetres away from the illuminator, then the laser scanner will outperform the LED one.

Moreover, a sex and age group specific subset analysis has been carried out which indicates that there is no substantial difference in terms of recognition performance for male and female subjects as well as among the different age groups of the subjects. Such a subgroup specific analysis has not been performed before. These results need further investigation and confirmation based on a larger data set.

As mentioned in the introduction, all the details about the scanner and its design will be made available as an open-hardware documentation together with an open-source repository where construction plans, schematics, parts lists, firmware, etc. can be found. Researchers can benefit from our open-source design, as it enables them to build a scanner based on our design on their own. By capturing and providing finger-vein images using a scanner based on our design, i.e. having essentially the same structure as we proposed, they can contribute to a large, open, publicly available finger-vein data set. The whole finger-vein research community will benefit from such a data set.

Together with our partners as well as other researchers building a scanner device based on our design, we are confident that our data set will continue to grow in the future. We are currently capturing further subjects in-house and our finger-vein data set is expected to contain more than 100 subjects by the end of 2018. Furthermore, we are extending our data set by capturing palmar finger-vein images as well, which will be released soon.

Acknowledgements

This project has received funding from the European Union’s Horizon 2020 research and innovation program under grant agreement No. 700259.

References

- [1] M. S. M. Asaari, S. A. Suandi, and B. A. Rosdi. Fusion of band limited phase only correlation and width centroid contour distance for finger based biometrics. *Expert Systems with Applications*, 41(7):3367–3382, 2014.
- [2] J. H. Choi, W. Song, T. Kim, S.-R. Lee, and H. C. Kim. Finger vein extraction using gradient normalization and principal curvature. volume 7251, pages 7251 – 7251 – 9, 2009.
- [3] S. Gabarda and G. Cristóbal. Blind image quality assessment through anisotropy. *JOSA A*, 24(12):B42–B51, 2007.
- [4] C. Kauba, J. Reissig, and A. Uhl. Pre-processing cascades and fusion in finger vein recognition. In *Proceedings of the International Conference of the Biometrics Special Interest Group (BIOSIG'14)*, Darmstadt, Germany, Sept. 2014.
- [5] J. Kim, H.-J. Kong, S. Park, S. Noh, S.-R. Lee, T. Kim, and H. C. Kim. Non-contact finger vein acquisition system using nir laser. In *Sensors, Cameras, and Systems for Industrial/Scientific Applications X*, volume 7249. International Society for Optics and Photonics, 2009.
- [6] A. Kumar and Y. Zhou. Human identification using finger images. *Image Processing, IEEE Transactions on*, 21(4):2228–2244, 2012.
- [7] L. Liu, B. Liu, H. Huang, and A. C. Bovik. No-reference image quality assessment based on spatial and spectral entropies. *Signal Processing: Image Communication*, 29(8):856–863, 2014.
- [8] D. G. Lowe. Object recognition from local scale-invariant features. In *Proceedings of the Seventh IEEE International Conference on Computer Vision (CVPR'99)*, volume 2, pages 1150 – 1157. IEEE, 1999.
- [9] Y. Lu, S. J. Xie, S. Yoon, Z. Wang, and D. S. Park. An available database for the research of finger vein recognition. In *Image and Signal Processing (CISP), 2013 6th International Congress on*, volume 1, pages 410–415. IEEE, 2013.
- [10] D. Maio, D. Maltoni, R. Cappelli, J. L. Wayman, and A. K. Jain. FVC2004: Third Fingerprint Verification Competition. In *ICBA*, volume 3072 of *LNCS*, pages 1–7. Springer Verlag, 2004.
- [11] K. Matkovic, L. Neumann, A. Neumann, T. Psik, and W. Purghofer. Global contrast factor-a new approach to image contrast. *Computational Aesthetics*, 2005:159–168, 2005.
- [12] N. Miura, A. Nagasaka, and T. Miyatake. Extraction of finger-vein patterns using maximum curvature points in image profiles. *IEICE transactions on information and systems*, 90(8):1185–1194, 2007.
- [13] R. Raghavendra and C. Busch. Exploring dorsal finger vein pattern for robust person recognition. In *2015 International Conference on Biometrics (ICB)*, pages 341–348, May 2015.
- [14] P. Tome, M. Vanoni, and S. Marcel. On the vulnerability of finger vein recognition to spoofing. In *IEEE International Conference of the Biometrics Special Interest Group (BIOSIG)*, Sept. 2014.
- [15] B. Ton and R. Veldhuis. A high quality finger vascular pattern dataset collected using a custom designed capturing device. In *International Conference on Biometrics, ICB 2013*. IEEE, 2013.
- [16] University of Reading. PROTECT Multimodal DB Dataset, June 2017. Available by request at <http://projectprotect.eu/dataset/>.
- [17] C. Wang, X. Zeng, X. Sun, W. Dong, and Z. Zhu. Quality assessment on near infrared palm vein image. In *Automation (YAC), 2017 32nd Youth Academic Annual Conference of Chinese Association of*, pages 1127–1130. IEEE, 2017.
- [18] W. Yang, X. Yu, and Q. Liao. Personal authentication using finger vein pattern and finger-dorsa texture fusion. In *Proceedings of the 17th ACM international conference on Multimedia*, pages 905–908. ACM, 2009.
- [19] Y. Yin, L. Liu, and X. Sun. Sdumla-hmt: a multimodal biometric database. *Biometric Recognition*, pages 260–268, 2011.
- [20] J. Zhang and J. Yang. Finger-vein image enhancement based on combination of gray-level grouping and circular gabor filter. In *Information Engineering and Computer Science, 2009. ICIECS 2009. International Conference on*, pages 1–4. IEEE, 2009.
- [21] J. Zhao, H. Tian, W. Xu, and X. Li. A new approach to hand vein image enhancement. In *Intelligent Computation Technology and Automation, 2009. ICICTA'09. Second International Conference on*, volume 1, pages 499–501. IEEE, 2009.
- [22] K. Zuiderveld. Contrast limited adaptive histogram equalization. In P. S. Heckbert, editor, *Graphics Gems IV*, pages 474–485. Morgan Kaufmann, 1994.